INTERNATIONAL JOURNAL FOR NUMERICAL METHODS IN FLUIDS
Int. J. Numer. Meth. Fluids 2008; **58**:861–877
Published online 17 March 2008 in Wiley InterScience (www.interscience.wiley.com). DOI: 10.1002/fld.1770

A continuous adjoint formulation for the computation of topological and surface sensitivities of ducted flows

C. Othmer*, †

Institute of Scientific Computing, Technical University of Braunschweig, Braunschweig, Germany

SUMMARY

Topology optimization of fluid dynamic systems is a comparatively young optimal design technique. Its central ingredient is the computation of topological sensitivity maps. Whereas, for finite element solvers, implementations of such sensitivity maps have been accomplished in the past, this study focuses on providing this functionality within a professional finite volume computational fluid dynamics solver. On the basis of a continuous adjoint formulation, we derive the adjoint equations and the boundary conditions for typical cost functions of ducted flows and present first results for two- and three-dimensional geometries. Emphasis is placed on the versatility of our approach with respect to changes in the objective function. We further demonstrate that surface sensitivity maps can also be computed with the implemented functionality and establish their connection with topological sensitivities. Copyright © 2008 John Wiley & Sons, Ltd.

Received 21 December 2006; Revised 11 December 2007; Accepted 1 January 2008

KEY WORDS: adjoint methods; sensitivities; topology optimization; shape optimization; ducted flows; finite volume solver

1. INTRODUCTION

Fluid dynamic optimal design problems are ubiquitous in the aerospace, automotive and marine industries. The developed methodologies range from bionic algorithms over gradient-based search to surrogate modelling. In the case of gradient-based optimization, the so-called adjoint method has long been identified as the method of choice for the computation of sensitivities. It allows for computing the complete gradient with the effort of only two solver calls—primal and adjoint—independent of the search space dimension. The success of this method is manifested by the large number of publications on adjoint-based optimization in fluid dynamics ([1–5] and references therein) and also in structure mechanics ([6] and references therein).

*Correspondence to: C. Othmer, Institute of Scientific Computing, Technical University of Braunschweig, Hans Sommer-Straße 65, 38902 Braunschweig, Germany.
†E-mail: c.othmer@tu-bs.de

While those works focused mostly on *shape* optimization of *external* aerodynamics, this study is dedicated to ducted flows. For this kind of flows, a very powerful optimization method recently emerged: fluid dynamic topology optimization [7]. Here, as opposed to conventional shape optimization, the geometry is not described via a parametrized surface, but with a volume mesh of the entire installation space. An adjoint method is then employed to compute whether a fluid cell is favourable or counterproductive for the flow in terms of the chosen cost function. After several iterations of punishing the identified counterproductive cells via a momentum loss term, which is commonly realized by individual cell porosities, the optimal topology finally emerges as a collection of non-punished volume cells.

The central ingredient for fluid dynamic topology optimization is the computation of topological sensitivities. For finite element solvers, a number of realizations of such a functionality exist already [8–13], extending the pioneering work of Borrvall and Petersson [7]. However, for the workhorse codes of industrial computational fluid dynamics (CFD), namely finite volume solvers, deriving topological sensitivity information for ducted flows has not yet gone beyond the level of proof-of-concept studies [14, 15]. The aim of this study is, therefore, to provide the theoretical basis for the implementation of sensitivity maps into a professional, finite volume CFD solver and to demonstrate its functioning with some instructive numerical examples.

The first question to be addressed when implementing an adjoint into a finite volume solver is whether to use the discrete or the continuous approach [16]: Following the continuous adjoint, one starts from the linearized primal equations in their *analytical* form, derives the adjoint equations analytically and then discretizes them to obtain the adjoint code. Alternatively, the discrete approach is operating on code level: It linearizes the *discretized* primal equations, transposes them and adds appropriate source terms in order to arrive at the adjoint code. This procedure can be automated to a certain degree by the so-called automatic differentiation techniques (e.g. [17, 18]).

The respective advantages and disadvantages of these two alternatives are the subject of ongoing discussions (see, e.g. [16] for a comparison), and we will not dwell on that any further. We opted for the continuous adjoint because of the following reasons: The software environment that we chose for the implementation (OpenFOAM—Open Field Operation And Manipulation [19]) offers object-oriented implementations of differential operators, which can be called upon on any kind of computational mesh and utilized in an abstract fashion. This makes the implementation of a continuous adjoint very straightforward [20]. In addition, by formulating the equations and boundary conditions in a way that can quickly be adapted to a broad range of objective functions, we were able to overcome the general disadvantage of the continuous approach of tedious code adaptations to different objective functions.

In the following, the theory underlying our implementation of a continuous adjoint into the professional finite volume solver OpenFOAM for the computation of sensitivities of ducted flows is presented. It constitutes the basis for all future extensions of this new functionality. A crucial component for continuous adjoints is the choice of the correct boundary conditions and their adaptation to different objective functions. To that end, special emphasis is placed on the derivation of the adjoint boundary conditions and to their versatility with respect to changes in the cost function. The paper is organized as follows: In Section 2, we first demonstrate how topological sensitivities can be computed via a continuous adjoint, derive the governing adjoint equations and boundary conditions, and show examples of topological sensitivities for two different cost functions. As a by-product of our implementation, the adjoint solver also allows one to compute surface sensitivities. This is presented in Section 3, which closes with an example of a surface sensitivity map computed by OpenFOAM.

DOI: 10.1002/fld

2. TOPOLOGICAL SENSITIVITIES

If J stands for the cost function to be minimized, the optimization problem can be stated as follows:

$$\text{minimize } J = J(\alpha, \mathbf{v}, p) \quad \text{subject to } \mathscr{R}(\alpha, \mathbf{v}, p) = 0 \tag{1}$$

where $\mathbf{v}$ and p stand for velocity and pressure, respectively, and α represents the design variables, i.e. the porosity distribution. $\mathscr{R} = (R_1, R_2, R_3, R_4)^{\mathrm{T}}$ denote the state equations, in our case the incompressible, steady-state Navier–Stokes equations:

$$(R_1, R_2, R_3)^{\mathrm{T}} = (\mathbf{v} \cdot \nabla)\mathbf{v} + \nabla p - \nabla \cdot (2\nu \mathsf{D}(\mathbf{v})) + \alpha \mathbf{v} \tag{2}$$

$$R_4 = -\nabla \cdot \mathbf{v} \tag{3}$$

with kinematic viscosity ν and the rate of strain tensor $\mathsf{D}(\mathbf{v}) = \frac{1}{2}(\nabla \mathbf{v} + (\nabla \mathbf{v})^{\mathrm{T}})$. In order to accommodate eddy viscosity turbulence models, we understand ν as the sum of molecular and turbulent viscosities. The inclusion of the Darcy term $\alpha \mathbf{v}$ allows for punishing counterproductive cells—the central component of topology optimization.

We thus have a constrained optimization problem, with the constraints being the state equations. Such problems are commonly tackled by introducing a Lagrange function L and reformulating the cost function as

$$L := J + \int_{\Omega} (\mathbf{u}, q) \mathscr{R} \, \mathrm{d}\Omega \tag{4}$$

where Ω stands for the flow domain. As Lagrange multipliers

$$(\mathbf{u}, q) = (u_1, u_2, u_3, q) \tag{5}$$

we have introduced the adjoint velocity $\mathbf{u}$ and the adjoint pressure q, respectively. For the desired sensitivities of the cost function w.r.t. the design variables α, we have to compute the total variation of L:

$$\delta L = \delta_{\alpha} L + \delta_{\mathbf{v}} L + \delta_p L \tag{6}$$

Since changes in α entail—by virtue of the state equations—variations of the flow field, the total variation of L also includes contributions from the changes in $\mathbf{v}$ and p. Computing the sensitivities straightaway from Equation (6) would therefore require to solve the state equations once for each design variable. If, however, the Lagrange multipliers $\mathbf{u}$ and q are chosen such that the variation w.r.t. the state variables vanishes identically,

$$\delta_{\mathbf{v}} L + \delta_p L = 0 \tag{7}$$

the sensitivities can be computed simply from

$$\delta L = \delta_{\alpha} L = \delta_{\alpha} J + \int_{\Omega} (\mathbf{u}, q) \delta_{\alpha} \mathscr{R} \, \mathrm{d}\Omega \tag{8}$$

which involves only relatively cheap derivatives w.r.t. α. This procedure thus constitutes an enormous saving in computational effort and is the central element of the so-called 'adjoint method' (see, e.g. [1–6]).

DOI: 10.1002/fld

Following Equation (8), the sensitivity of the cost function w.r.t. the porosity α_i of cell i can be computed as

$$\frac{\partial L}{\partial \alpha_i} = \frac{\partial J}{\partial \alpha_i} + \int_\Omega (\mathbf{u}, q) \frac{\partial \mathscr{R}}{\partial \alpha_i} \, \mathrm{d}\Omega \tag{9}$$

For the methodology of topology optimization, the porosity is just an auxiliary variable to describe a continuous transition from fluid to solid, and usually there is no *explicit* dependence of the cost function on the porosity: $\partial J / \partial \alpha_i = 0$. Furthermore, as the porosity α_i enters the primal equation system only in cell i and only via the Darcy term, we can express

$$\frac{\partial \mathscr{R}}{\partial \alpha_i} = \begin{pmatrix} \mathbf{v} \\ 0 \end{pmatrix} \chi_i \tag{10}$$

with χ_i being the characteristic function of cell i. According to Equation (9), we can finally compute the desired sensitivity for each cell as the dot product of adjoint and primal velocity times the cell volume:

$$\frac{\partial L}{\partial \alpha_i} = \mathbf{u}_i \cdot \mathbf{v}_i V_i \tag{11}$$

Hence, in order to compute topological sensitivities, all we need apart from the primal solution is the adjoint velocity distribution $\mathbf{u}$. As stated above, the adjoint quantities $\mathbf{u}$ and q are defined by the requirement that the state variable contribution to the variation of L vanishes. The governing equation system for the adjoint variables and their boundary conditions are therefore to be derived from Equation (7), which will be done in the following section.

2.1. Derivation of adjoint equations and boundary conditions

The starting point for the derivation of the adjoint equation system is Equation (7)—the vanishing of the variation of L w.r.t. the state variables. Following the definition of the Lagrange function, Equation (4), this requirement reads

$$\delta_{\mathbf{v}} J + \delta_p J + \int_\Omega (\mathbf{u}, q) \delta_{\mathbf{v}} \mathscr{R} \, \mathrm{d}\Omega + \int_\Omega (\mathbf{u}, q) \delta_p \mathscr{R} \, \mathrm{d}\Omega = 0 \tag{12}$$

If the state equations $\mathscr{R}$ are the incompressible Navier–Stokes equations (2) and (3), the derivatives w.r.t. $\mathbf{v}$ and p can be computed straightforwardly as

$$\delta_{\mathbf{v}} (R_1, R_2, R_3)^{\mathrm{T}} = (\delta \mathbf{v} \cdot \nabla) \mathbf{v} + (\mathbf{v} \cdot \nabla) \delta \mathbf{v} - \nabla \cdot (2\nu \mathsf{D}(\delta \mathbf{v})) + \alpha \delta \mathbf{v} \tag{13}$$

$$\delta_{\mathbf{v}} R_4 = -\nabla \cdot \delta \mathbf{v} \tag{14}$$

$$\delta_p (R_1, R_2, R_3)^{\mathrm{T}} = \nabla \delta p \tag{15}$$

$$\delta_p R_4 = 0 \tag{16}$$

Here, we have neglected the variation of the eddy viscosity ν. This is correct only for laminar flow regimes. For turbulent flows, neglecting this variation constitutes a common approximation,

DOI: 10.1002/fld

which is known as 'frozen turbulence' [21]. With these derivatives, Equation (12) now reads

$$\delta_{\mathbf{v}} J + \delta_p J + \int_\Omega \mathrm{d}\Omega \mathbf{u} \cdot ((\delta\mathbf{v} \cdot \nabla)\mathbf{v} + (\mathbf{v} \cdot \nabla)\delta\mathbf{v} - \nabla \cdot (2\nu \mathsf{D}(\delta\mathbf{v})) + \alpha\delta\mathbf{v}) - \int_\Omega \mathrm{d}\Omega q \nabla \cdot \delta\mathbf{v} + \int_\Omega \mathrm{d}\Omega \mathbf{u} \cdot \nabla \delta p = 0 \tag{17}$$

After integration by parts and decomposition of the cost function J into contributions from the boundary $\Gamma = \partial\Omega$ and from the interior of Ω,

$$J = \int_\Gamma J_\Gamma \, \mathrm{d}\Gamma + \int_\Omega J_\Omega \, \mathrm{d}\Omega \tag{18}$$

we can finally reformulate Equation (17) as follows:

$$\begin{aligned} &\int_\Gamma \mathrm{d}\Gamma \left(\mathbf{u} \cdot \mathbf{n} + \frac{\partial J_\Gamma}{\partial p} \right) \delta p + \int_\Omega \mathrm{d}\Omega \left(-\nabla \cdot \mathbf{u} + \frac{\partial J_\Omega}{\partial p} \right) \delta p \\ &+ \int_\Gamma \mathrm{d}\Gamma \left(\mathbf{n}(\mathbf{u} \cdot \mathbf{v}) + \mathbf{u}(\mathbf{v} \cdot \mathbf{n}) + 2\nu \mathbf{n} \cdot \mathsf{D}(\mathbf{u}) - q\mathbf{n} + \frac{\partial J_\Gamma}{\partial \mathbf{v}} \right) \cdot \delta\mathbf{v} - \int_\Gamma \mathrm{d}\Gamma 2\nu \mathbf{n} \cdot \mathsf{D}(\delta\mathbf{v}) \cdot \mathbf{u} \\ &+ \int_\Omega \mathrm{d}\Omega \left(-\nabla\mathbf{u} \cdot \mathbf{v} - (\mathbf{v} \cdot \nabla)\mathbf{u} - \nabla \cdot (2\nu \mathsf{D}(\mathbf{u})) + \alpha\mathbf{u} + \nabla q + \frac{\partial J_\Omega}{\partial \mathbf{v}} \right) \cdot \delta\mathbf{v} = 0 \end{aligned} \tag{19}$$

This equation has to be fulfiled for any $\delta\mathbf{v}$ and δp that satisfy the primal Navier–Stokes equations, which can in general be accomplished only if the integrals vanish individually. For the integrals over the domain, this requirement gives rise to the adjoint equations, whereas the adjoint boundary conditions can be deduced from the vanishing of the boundary integrals.

From Equation (19), we thus derive the adjoint Navier–Stokes equations as follows:

$$-2\mathsf{D}(\mathbf{u})\mathbf{v} = -\nabla q + \nabla \cdot (2\nu \mathsf{D}(\mathbf{u})) - \alpha\mathbf{u} - \frac{\partial J_\Omega}{\partial \mathbf{v}} \tag{20}$$

$$\nabla \cdot \mathbf{u} = \frac{\partial J_\Omega}{\partial p} \tag{21}$$

where we have expressed $-\nabla\mathbf{u} \cdot \mathbf{v} - (\mathbf{v} \cdot \nabla)\mathbf{u}$ as $-2\mathsf{D}(\mathbf{u})\mathbf{v}$.

As boundary conditions for adjoint velocity and pressure, we deduce from Equation (19) that

$$\int_\Gamma \mathrm{d}\Gamma \left(\mathbf{n}(\mathbf{u} \cdot \mathbf{v}) + \mathbf{u}(\mathbf{v} \cdot \mathbf{n}) + 2\nu \mathbf{n} \cdot \mathsf{D}(\mathbf{u}) - q\mathbf{n} + \frac{\partial J_\Gamma}{\partial \mathbf{v}} \right) \cdot \delta\mathbf{v} - \int_\Gamma \mathrm{d}\Gamma 2\nu \mathbf{n} \cdot \mathsf{D}(\delta\mathbf{v}) \cdot \mathbf{u} = 0 \tag{22}$$

$$\int_\Gamma \mathrm{d}\Gamma \left(\mathbf{u} \cdot \mathbf{n} + \frac{\partial J_\Gamma}{\partial p} \right) \delta p = 0 \tag{23}$$

This is the general form of the adjoint equation system for the steady-state, incompressible Navier–Stokes equations with Darcy porosity and frozen turbulence. Albeit linear by definition, the structure of the adjoint Navier–Stokes equations is very similar to that of the primal

DOI: 10.1002/fld

equations. Moreover, a large variety of cost functions for ducted as well as external flows, such as pressure drop or drag, are surface integrals over the domain boundary. They do not contain a contribution from the domain interior ($J_\Omega = 0$). Hence, for this type of objective function, the adjoint flow field is also divergenceless, much as the primal one. The dominant difference between primal and adjoint equations is, however, the minus sign in front of the convective term of Equation (20). It states that adjoint information is convected upstream of the primal flow rather than downstream.

2.2. *Specialization to ducted flows*

After having derived the general form of the adjoint equations and boundary conditions, this section is dedicated to their specialization to ducted flows. For this kind of flow regimes, the flow domain boundary Γ is made up of three portions—inlet, outlet and wall, where the following conditions are commonly imposed on the state variables: prescribed velocity and zero pressure gradient in the inlet, zero velocity gradient and zero pressure at the outlet, and a no-slip condition and zero pressure gradient along the wall.

As already stated above, typical objective functions of ducted flows involve only integrals over the surface of the flow domain rather than over its interior. In that case, the adjoint equations (20) and (21) reduce to

$$-2\mathsf{D}(\mathbf{u})\mathbf{v} = -\nabla q + \nabla\cdot(2\nu\mathsf{D}(\mathbf{u})) - \alpha\mathbf{u} \tag{24}$$

$$\nabla\cdot\mathbf{u} = 0 \tag{25}$$

Note that the adjoint equation system does not depend on the cost function anymore. Therefore, when switching from one optimization objective to another, the solver remains unchanged, and only the boundary conditions have to be adapted to the specific cost function.

Before we discuss the adjoint boundary conditions in detail, we will elaborate a bit on the boundary terms of Equation (22) that involve the rate of strain tensor D. For divergenceless fields $\delta\mathbf{v}$ and $\mathbf{u}$ with at least one of them vanishing on $\partial\Gamma$, it can be shown that the following relation holds:

$$\begin{aligned}\int_\Gamma \mathrm{d}\Gamma 2\nu\mathbf{n}\cdot(\mathsf{D}(\mathbf{u})\cdot\delta\mathbf{v} - \mathsf{D}(\delta\mathbf{v})\cdot\mathbf{u}) = \int_\Gamma \mathrm{d}\Gamma \nu((\mathbf{n}\cdot\nabla)\mathbf{u}\cdot\delta\mathbf{v} - (\mathbf{n}\cdot\nabla)\delta\mathbf{v}\cdot\mathbf{u}) \\ - \int_\Gamma \mathrm{d}\Gamma\nabla\nu\cdot(u_n\delta\mathbf{v} - \delta v_n\mathbf{u})\end{aligned} \tag{26}$$

where $u_n = \mathbf{u}\cdot\mathbf{n}$ and $v_n = \mathbf{v}\cdot\mathbf{n}$ are the normal components of adjoint and primal velocities, respectively.

For laminar flows, ν contains only the molecular viscosity, and its gradient obviously vanishes. Still for turbulent flows, $\nabla\nu = 0$ along the wall and—for homogeneously prescribed degrees of turbulence—also at the inlet. In the outlet area, $\nabla\nu$ is in general non-zero. However, we assume its product with the difference term in brackets in Equation (26) to be of second order. For the remainder of the derivation, we will therefore neglect the second integral of Equation (26).

DOI: 10.1002/fld

Boundary conditions (22) and (23) then reduce to

$$\int_\Gamma \mathrm{d}\Gamma \left(\mathbf{n}(\mathbf{u}\cdot\mathbf{v}) + \mathbf{u}(\mathbf{v}\cdot\mathbf{n}) + \nu(\mathbf{n}\cdot\nabla)\mathbf{u} - q\mathbf{n} + \frac{\partial J_\Gamma}{\partial \mathbf{v}} \right) \cdot \delta\mathbf{v} - \int_\Gamma \mathrm{d}\Gamma \nu(\mathbf{n}\cdot\nabla)\delta\mathbf{v}\cdot\mathbf{u} = 0 \tag{27}$$

$$\int_\Gamma \mathrm{d}\Gamma \left(\mathbf{u}\cdot\mathbf{n} + \frac{\partial J_\Gamma}{\partial p} \right) \delta p = 0 \tag{28}$$

These conditions will now be evaluated for the inlet, wall and outlet portions of the domain boundary, in order to deduce the boundary conditions for the adjoint variables, thereby making use of the fact that the admissible perturbations $\delta\mathbf{v}$ and δp are such that the perturbed quantities $\mathbf{v}+\delta\mathbf{v}$ and $p+\delta p$ satisfy the primal equation system.

2.2.1. Wall and inlet. On these parts of Γ, the primal velocity is usually fixed: to zero (no-slip condition on the wall) and to its prescribed value at the inlet, respectively. We therefore have $\delta\mathbf{v}=0$ here, and the first integral of Equation (27) cancels. From

$$0 = \nabla\cdot\delta\mathbf{v} = (\mathbf{n}\cdot\nabla)\delta v_n + \nabla_\parallel \cdot \delta\mathbf{v}_t \tag{29}$$

and $\delta\mathbf{v}_t = 0$ along the wall and inlet—with $\nabla_\parallel$ and $\mathbf{v}_t$ being the in-plane components of ∇ and $\mathbf{v}$, respectively—we conclude that

$$(\mathbf{n}\cdot\nabla)\delta v_n = 0 \tag{30}$$

and hence

$$(\mathbf{n}\cdot\nabla)\delta\mathbf{v} = (\mathbf{n}\cdot\nabla)\delta\mathbf{v}_t \tag{31}$$

Equations (27) and (28) thus reduce to

$$\int_\Gamma \mathrm{d}\Gamma \nu(\mathbf{n}\cdot\nabla)\delta\mathbf{v}_t\cdot\mathbf{u}_t = 0 \tag{32}$$

$$\int_\Gamma \mathrm{d}\Gamma \left(\mathbf{u}\cdot\mathbf{n} + \frac{\partial J_\Gamma}{\partial p} \right) \delta p = 0 \tag{33}$$

from which we conclude the boundary conditions for the adjoint velocity at the wall and inlet:

$$\mathbf{u}_t = 0 \tag{34}$$

$$u_n = -\frac{\partial J_\Gamma}{\partial p} \tag{35}$$

Note that these derivations do not impose a condition for the adjoint pressure q. Since the adjoint pressure q enters the adjoint Navier–Stokes equations in a similar way as its primal counterpart p enters the primal Navier–Stokes equations, the zero gradient boundary condition of p at the wall and inlet is applied to q as well, in order to assure the well posedness of the adjoint equation system.

DOI: 10.1002/fld

2.2.2. Outlet. The typical primal outlet conditions are zero velocity gradient and zero pressure:

$$(\mathbf{n}\cdot\nabla)\delta\mathbf{v} \quad \text{and} \quad p=0 \tag{36}$$

The second integral of Equation (27) therefore cancels, and with $\delta p=0$ Equation (28) is identically fulfilled. The only remaining term is thus the first integral of Equation (27), which can be made to cancel by enforcing the integrand to vanish:

$$\mathbf{n}(\mathbf{u}\cdot\mathbf{v})+\mathbf{u}(\mathbf{v}\cdot\mathbf{n})+\nu(\mathbf{n}\cdot\nabla)\mathbf{u}-q\mathbf{n}+\frac{\partial J_\Gamma}{\partial\mathbf{v}}=0 \tag{37}$$

Decomposition of Equation (37) into its normal and tangential components yields

$$\mathbf{u}\cdot\mathbf{v}+u_n v_n+\nu(\mathbf{n}\cdot\nabla)u_n-q+\frac{\partial J_\Gamma}{\partial v_n}=0 \tag{38}$$

$$v_n\mathbf{u}_t+\nu(\mathbf{n}\cdot\nabla)\mathbf{u}_t+\frac{\partial J_\Gamma}{\partial\mathbf{v}_t}=0 \tag{39}$$

The normal component (38) can be satisfied by choosing the adjoint pressure q accordingly

$$q=\mathbf{u}\cdot\mathbf{v}+u_n v_n+\nu(\mathbf{n}\cdot\nabla)u_n+\frac{\partial J_\Gamma}{\partial v_n} \tag{40}$$

whereas the tangential component (39) is used to determine the tangential component of the adjoint velocity $\mathbf{u}_t$. For the gradient of the normal component u_n, continuity then implies that

$$(\mathbf{n}\cdot\nabla)u_n=\nabla\cdot\mathbf{u}-\nabla_\parallel\cdot\mathbf{u}_t=-\nabla_\parallel\cdot\mathbf{u}_t \tag{41}$$

This completes the adjoint boundary conditions for ducted flows. Before we evaluate them in the following two sections for two cost function examples, let us summarize the findings of our derivation—the adjoint Navier–Stokes equations and the adjoint boundary conditions for ducted flow optimization:

Adjoint Navier–Stokes equations:

$$-2\mathsf{D}(\mathbf{u})\mathbf{v}=-\nabla q+\nabla\cdot(2\nu\mathsf{D}(\mathbf{u}))-\alpha\mathbf{u} \tag{42}$$

$$\nabla\cdot\mathbf{u}=0 \tag{43}$$

Adjoint boundary conditions for the wall and inlet:

$$\mathbf{u}_t=0 \tag{44}$$

$$u_n=-\frac{\partial J_\Gamma}{\partial p} \tag{45}$$

$$\mathbf{n}\cdot\nabla q=0 \tag{46}$$

Adjoint boundary conditions for the outlet:

$$q=\mathbf{u}\cdot\mathbf{v}+u_n v_n+\nu(\mathbf{n}\cdot\nabla)u_n+\frac{\partial J_\Gamma}{\partial v_n} \tag{47}$$

$$0=v_n\mathbf{u}_t+\nu(\mathbf{n}\cdot\nabla)\mathbf{u}_t+\frac{\partial J_\Gamma}{\partial\mathbf{v}_t} \tag{48}$$

DOI: 10.1002/fld

2.3. *Example 1*: *Dissipated power*

The power dissipated by a fluid dynamic device can be computed as the net inward flux of energy, i.e. total pressure, through the device boundaries:

$$J := -\int_\Gamma \mathrm{d}\Gamma \left(p + \frac{1}{2} v^2 \right) \mathbf{v} \cdot \mathbf{n} \tag{49}$$

For this cost function, we obviously have

$$J_\Omega = 0 \quad \text{and} \quad J_\Gamma = -(p + \tfrac{1}{2} v^2) \mathbf{v} \cdot \mathbf{n} \tag{50}$$

The derivatives needed for the boundary conditions are

$$\frac{\partial J_\Gamma}{\partial p} = -\mathbf{v} \cdot \mathbf{n} \quad \text{and} \quad \frac{\partial J_\Gamma}{\partial \mathbf{v}} = -(p + \tfrac{1}{2} v^2) \mathbf{n} - (\mathbf{v} \cdot \mathbf{n}) \mathbf{v} \tag{51}$$

From Equations (44) and (45), we thus obtain for the adjoint velocity at the wall and inlet

$$\mathbf{u}_t = 0 \tag{52}$$

$$u_n = \begin{cases} 0 & \text{at wall} \\ v_n & \text{at inlet} \end{cases} \tag{53}$$

whereas according to Equations (47) and (48), the outlet conditions are

$$q = \mathbf{u} \cdot \mathbf{v} + u_n v_n + \nu (\mathbf{n} \cdot \nabla) u_n - \tfrac{1}{2} v^2 - v_n^2 \tag{54}$$

$$0 = v_n (\mathbf{u}_t - \mathbf{v}_t) + \nu (\mathbf{n} \cdot \nabla) \mathbf{u}_t \tag{55}$$

Figure 1 illustrates the sensitivities thus obtained for a simple two-dimensional (2D) test case with 100×100 Cartesian grid cells. At a Reynolds number of 1000, the flow enters the box through an inlet on the south wall and leaves it through an outlet on the east wall. The sensitivities of the cells that are favourable for the flow (i.e. those with positive values of $\partial J / \partial \alpha_i$) and the counterproductive cells are shown separately in Figures 1(a) and (b). As expected, the most important cells for the flow passage lie along the main path, whereas the most prominent counterproductive cells are located in the main backflow region.

The sensitivity distributions of Figure 1 reproduce those of Othmer *et al*. [15], who applied an AD-based adjoint code to the same geometry (their Figure 3), and a finite difference check of the sensitivities (Figure 2) confirms the validity of the implementation. The inaccuracies of the adjoint-based sensitivities as apparent from Figure 2 are presumably caused by the approximations in the adjoint derivation (i.e. neglecting the second-order term in Equation (26)) and the frozen turbulence assumption. For a detailed quantitative study of the effect of frozen turbulence on the accuracy of adjoint-based gradients, we refer to the recent work by Dwight and Brezillon [21].

How such topological sensitivity maps can be employed in conjunction with a gradient-based algorithm for the topological optimization of fluid dynamic problems was already demonstrated [8–12]. Those works identified Svanberg's method of moving asymptotes [22] as being highly efficient for this kind of optimization problems. For an in-depth study of the optimization itself, we therefore refer to those studies and rather focus on the computation of sensitivities for a second cost function.

DOI: 10.1002/fld

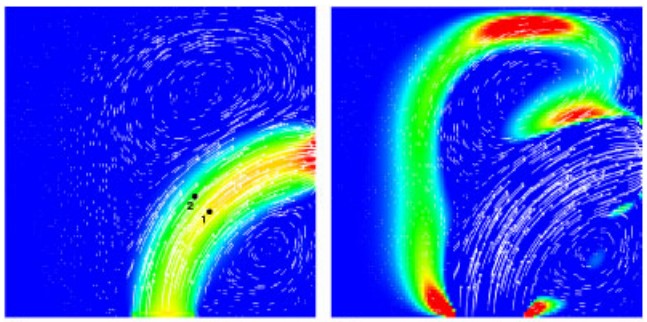

Figure 1. Box test case for dissipated power: (a) sensitivities of favourable cells and (b) sensitivities of counterproductive cells. The dots in (a) depict the locations of the finite difference check of Figure 2.

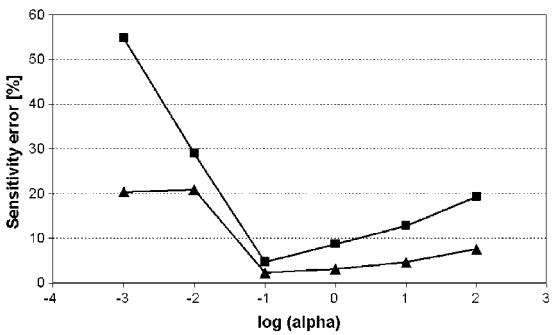

Figure 2. Finite difference check of computed sensitivities: magnitude of the relative error between adjoint-based sensitivities and those computed via finite differences for various values of the step size α (squares: point 1 of Figure 1(a), triangles: point 2). A step size of $\alpha = 0.1$ appears to be a good choice, as below, the round-off error becomes dominant.

2.4. *Example 2: Flow uniformity at the outlet*

Apart from the dissipated power, the uniformity of the flow upon leaving the outlet plane is an important design criterion of, e.g. automotive air ducts. It is related to the efficiency of distributing fresh air inside the car and thus to passenger comfort. This objective can be captured by a cost function of the form:

$$J := \int_{\text{outlet}} \mathrm{d}\Gamma \frac{c}{2}(\mathbf{v} - \mathbf{v}^{\mathrm{d}})^2 \tag{56}$$

where $\mathbf{v}^{\mathrm{d}}$ is the desired velocity in the outlet plane and $c = 1\,\mathrm{m}^{-2}\,\mathrm{s}^{-1}$ is a constant used for unit consistency. There is no contribution to the cost function either from the domain itself or from the

DOI: 10.1002/fld

inlet and wall:

$$J_\Omega = 0 \tag{57}$$

$$J_\Gamma = \begin{cases} 0 & \text{at wall and inlet} \\ \dfrac{c}{2}(\mathbf{v}-\mathbf{v}^{\mathrm{d}})^2 & \text{at outlet} \end{cases} \tag{58}$$

Consequently, we obtain $\mathbf{u}=0$ as the velocity boundary condition for the wall and inlet. For the outlet, we compute the required derivatives as

$$\frac{\partial J_\Gamma}{\partial v_n} = c(v_n - v_n^{\mathrm{d}}) \quad \text{and} \quad \frac{\partial J_\Gamma}{\partial \mathbf{v}_t} = c(\mathbf{v}_t - \mathbf{v}_t^{\mathrm{d}}) \tag{59}$$

and arrive according to Equations (47) and (48) at the following boundary conditions:

$$q = \mathbf{u}\cdot\mathbf{v} + u_n v_n + \nu(\mathbf{n}\cdot\nabla)u_n + c(v_n - v_n^{\mathrm{d}}) \tag{60}$$

$$0 = v_n \mathbf{u}_t + \nu(\mathbf{n}\cdot\nabla)\mathbf{u}_t + c(\mathbf{v}_t - \mathbf{v}_t^{\mathrm{d}}) \tag{61}$$

Note that the difference between actual and desired velocities $\mathbf{v}-\mathbf{v}^{\mathrm{d}}$ acts as a 'source term' in the outlet boundary conditions.

For the 2D box example of the previous section, Figure 3(a) shows the sensitivities obtained in this way. The desired outlet velocity was chosen to be $\mathbf{v}^{\mathrm{d}} = (v_x^{\mathrm{d}}, v_y^{\mathrm{d}})^{\mathrm{T}} = (1,0)^{\mathrm{T}}$. The stripe in Figure 3(b) displays the deviation from the optimal velocity distribution along the eastern boundary, i.e. the difference $\Delta v_n := v_n - v_n^{\mathrm{d}}$ between actual and desired velocities. As expected, the cells along the flow lines with above-average outlet velocities ($\Delta v_n > 0$, blue in Figure 3(b)) have negative sensitivities ($\partial J/\partial\alpha < 0$, blue in Figure 3(a)); in other words, their punishment via a finite porosity would improve the uniformity. Conversely, the cells with positive sensitivities (red) are located on flow lines with below-average outlet velocities.

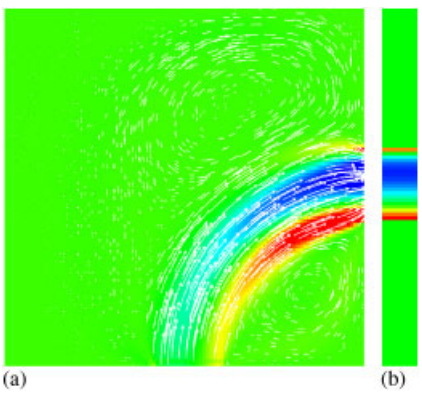

Figure 3. Box test case for outlet flow uniformity: (a) flow field and sensitivities (blue: $\partial J/\partial\alpha < 0$, i.e. their punishment improves the uniformity, red: $\partial J/\partial\alpha > 0$, green: sensitivity close to zero) and (b) the deviation from uniformity, $\Delta v_n = v_n - v_n^{\mathrm{d}}$, taken along the eastern wall (blue: $\Delta v_n > 0$, red: $\Delta v_n < 0$).

DOI: 10.1002/fld

3. SURFACE SENSITIVITIES

In the preceding sections, we have introduced an adjoint-based methodology for the computation of topological sensitivities. The fact that such sensitivities represent an efficient tool for generating optimal duct designs was demonstrated in several publications [8–15]. An inherent feature of topology optimization is, however, the ragged surface of the resulting geometries. A CFD computation on such a geometry can obviously not be as accurate as on a body-fitted mesh. Therefore, the virtue of topology optimization lies rather in the efficient *drafting* of designs than in geometrical *fine-tuning*. For the latter, optimization methodologies operating directly on the shape have to be employed. With a view to maximizing the design freedom, allowed shape modifications can efficiently be described as a superposition of localized surface normal displacements β, an idea first introduced by Pironneau [23]. The cost function variation incurred by such perturbations can be computed analogously to Equation (8) as

$$\delta_\beta L = \delta_\beta J + \delta_\beta \int_\Omega (\mathbf{u}, q)\mathscr{R}\,\mathrm{d}\Omega \tag{62}$$

where $\mathscr{R}$ stands again for the residuals of the Navier–Stokes equations (2) and (3), omitting, however, the Darcy term, which is not needed for shape optimization.

The first term of Equation (62) represents the explicit dependence of the cost function on the design variables. If the objective function involves integrals over the surface that is to be optimized, this term does not vanish—as opposed to the case of topological optimization (cf. Section 2). It can, however, be computed in a straightforward manner by purely geometric considerations on the primal flow field. The evaluation of the second term of Equation (62) is more elaborate: It requires not only the adjoint solution but also metrics information for the evaluation of the impact of surface perturbations on the Navier–Stokes residuals [4]. A 'metrics-free' and therefore more straightforward methodology of computing this term was introduced by Soto and Löhner [5]: They recast the volume integral of Equation (62) as a boundary integral and, thus, reduce the computation of this term to a pure post-processing of the primal and the adjoint fields. As will be shown in the following, this intriguing methodology allows us to compute surface sensitivities from the very same results that are required for the computation of topological sensitivities.

By making use of the fact that for any admissible variation of $\mathbf{v}$ and p the total variation of $\mathscr{R}$ vanishes,

$$\delta\mathscr{R} = 0 \;\Leftrightarrow\; \delta_\beta\mathscr{R} + \delta_{\mathbf{v}}\mathscr{R} + \delta_p\mathscr{R} = 0 \tag{63}$$

we can recast the sensitivity of Equation (62) as follows:

$$\delta_\beta L = \delta_\beta J - \int_\Omega (\mathbf{u}, q)\delta_{\mathbf{v}}\mathscr{R}\,\mathrm{d}\Omega - \int_\Omega (\mathbf{u}, q)\delta_p\mathscr{R}\,\mathrm{d}\Omega \tag{64}$$

The last two integrals already showed up in the derivation of the adjoint equations (see Equation (12)). Besides the terms involving the cost function, they actually make up the adjoint equation system. For the reformulation of these terms, we can therefore directly take over the results obtained in Equation (19) of Section 2.1 and just leave out the cost function

DOI: 10.1002/fld

contribution:

$$\delta_\beta L = \delta_\beta J - \int_\Gamma \mathrm{d}\Gamma \mathbf{u}\cdot\mathbf{n}\delta p + \int_\Omega \mathrm{d}\Omega \nabla\cdot\mathbf{u}\delta p - \int_\Gamma \mathrm{d}\Gamma(\mathbf{n}(\mathbf{u}\cdot\mathbf{v}) + \mathbf{u}(\mathbf{v}\cdot\mathbf{n}) + 2\nu\mathbf{n}\cdot\mathsf{D}(\mathbf{u}) - q\mathbf{n})\cdot\delta\mathbf{v}$$
$$+ \int_\Gamma \mathrm{d}\Gamma 2\nu\mathbf{n}\cdot\mathsf{D}(\delta\mathbf{v})\cdot\mathbf{u} - \int_\Omega \mathrm{d}\Omega(-\nabla\mathbf{u}\cdot\mathbf{v} - (\mathbf{v}\cdot\nabla)\mathbf{u} - \nabla\cdot(2\nu\mathsf{D}(\mathbf{u})) + \nabla q)\cdot\delta\mathbf{v} \tag{65}$$

If the objective function does not depend on the domain interior ($J_\Omega = 0$), the volume terms of Equation (65) cancel by virtue of $\mathbf{u}$ and q satisfying the adjoint equations (42) and (43). We thus arrive at the following expression for the variation $\delta_\beta L$:

$$\delta_\beta L = \delta_\beta J - \int_\Gamma \mathrm{d}\Gamma \mathbf{u}\cdot\mathbf{n}\delta p - \int_\Gamma \mathrm{d}\Gamma(\mathbf{n}(\mathbf{u}\cdot\mathbf{v}) + \mathbf{u}(\mathbf{v}\cdot\mathbf{n})$$
$$+ 2\nu\mathbf{n}\cdot\mathsf{D}(\mathbf{u}) - q\mathbf{n})\cdot\delta\mathbf{v} + \int_\Gamma \mathrm{d}\Gamma 2\nu\mathbf{n}\cdot\mathsf{D}(\delta\mathbf{v})\cdot\mathbf{u} \tag{66}$$

For any objective function with $J_\Omega = 0$, this is an *exact* formulation of $\delta_\beta L$.[‡] In this form, however, it does not serve for a computation of the desired sensitivities, since $\delta\mathbf{v}$ and δp are unknown. We therefore have to find an *approximation* for these quantities. As the geometrical deformations controlled by our design variables β are in normal direction only, we follow the suggestion of Soto and Löhner [5] and make a Taylor series expansion for $\delta\mathbf{v}$ and δp:

$$\delta\mathbf{v} = \beta(\mathbf{n}\cdot\nabla)\mathbf{v} + \mathcal{O}(\beta^2) \quad \text{and} \quad \delta p = \beta(\mathbf{n}\cdot\nabla)p + \mathcal{O}(\beta^2) \tag{67}$$

Terminating the expansion after the linear term and substituting it into Equation (66) then allows for computing the desired sensitivities. What they look like for ducted flows will be derived in the remainder of this section.

For ducted flow optimization with fixed inlet and outlet geometries, the only portion of Γ that is subject to shape deformations $\beta \neq 0$ is obviously the wall. Conversely, the typical cost functions of ducted flows do not usually involve the flow quantities on the wall,[§] but are rather formulated as integrals over inlet and/or outlet. This has two implications: There is no explicit dependence of the cost function on the deformation, $\partial J/\partial\beta = 0$, and from Equations (44) and (45) we conclude that $\mathbf{u} = 0$ on the wall. Equation (66) therefore reduces to

$$\delta_\beta L = -\int_{\text{wall}} \mathrm{d}\Gamma(2\nu\mathbf{n}\cdot\mathsf{D}(\mathbf{u}) - q\mathbf{n})\cdot\beta(\mathbf{n}\cdot\nabla)\mathbf{v} \tag{68}$$

In order to simplify that expression, we express $2\mathbf{n}\cdot\mathsf{D}(\mathbf{u})$ as

$$2\mathbf{n}\cdot\mathsf{D}(\mathbf{u}) = (\mathbf{n}\cdot\nabla)\mathbf{u} + \nabla(\mathbf{u}\cdot\mathbf{n}) \tag{69}$$

[‡]Note that the boundary integrals of Equation (66) correspond to those of the adjoint boundary conditions (22) and (23)—*without*, however, the cost function contributions. Therefore, another way of arriving at Equation (66) is as follows: Write the total variation as $\delta_\beta L = \delta_\beta J + \delta_\mathbf{v} J + \delta_p J$ and replace the variations w.r.t. $\mathbf{v}$ and p by virtue of the adjoint boundary conditions (22) and (23).

[§]If this was, however, the case, i.e. if the objective function was formulated as an integral over the wall, one would better fall back on the so-called *incomplete* sensitivities anyway, which do not necessitate an adjoint solution at all [3, 24].

DOI: 10.1002/fld

With $\nabla\cdot\mathbf{u}=0$ in Ω and $\mathbf{u}=0$ at the wall, we follow the reasoning that lead to Equation (30) and conclude that

$$(\mathbf{n}\cdot\nabla)u_n=0 \tag{70}$$

Using again that $u_n=0$ along the wall, we further note that the second term of Equation (69) cancels:

$$\nabla(\mathbf{u}\cdot\mathbf{n})=\mathbf{n}(\mathbf{n}\cdot\nabla)u_n+\nabla_{\|}u_n=0 \tag{71}$$

We thus arrive at

$$2\mathbf{n}\cdot\mathsf{D}(\mathbf{u})=(\mathbf{n}\cdot\nabla)\mathbf{u}_t \tag{72}$$

Similarly,

$$(\mathbf{n}\cdot\nabla)\mathbf{v}=(\mathbf{n}\cdot\nabla)\mathbf{v}_t \tag{73}$$

and since

$$\mathbf{n}\cdot((\mathbf{n}\cdot\nabla)\mathbf{v}_t)=0 \tag{74}$$

we can finally express the variation of L as

$$\delta_\beta L=-\int_{\text{wall}}\mathrm{d}\Gamma\beta v(\mathbf{n}\cdot\nabla)\mathbf{u}_t\cdot(\mathbf{n}\cdot\nabla)\mathbf{v}_t \tag{75}$$

The desired sensitivity for an outward movement β at some specific point of the surface is thus

$$\frac{\partial L}{\partial\beta}=-Av(\mathbf{n}\cdot\nabla)\mathbf{u}_t\cdot(\mathbf{n}\cdot\nabla)\mathbf{v}_t \tag{76}$$

with A being the surface area affected by this movement. In other words, the surface sensitivities can be obtained as the dot product of the normal gradients of primal and adjoint velocities.

We emphasize again that the prerequisites for a computation of topological and surface sensitivities are actually the same: the primal and the adjoint velocity fields. Once these fields are obtained, both types of sensitivities can be computed—by multiplying either the velocities themselves in the interior of the domain (Equation (11)) or their normal gradients at the domain boundary (Equation (76)). It is now instructive to have a closer look at the connection between the two sensitivity types at the wall: An inward displacement $\beta<0$ of the surface produces, according to Equation (75), a variation of the objective function of

$$\mathrm{d}L_{\text{surf}}\propto(\mathbf{n}\cdot\nabla)\mathbf{u}_t\cdot(\mathbf{n}\cdot\nabla)\mathbf{v}_t \tag{77}$$

As $\mathbf{u}_t=0$ at the wall, we can approximate for sufficiently small displacements β:

$$(\mathbf{n}\cdot\nabla)\mathbf{u}_t\approx|\beta|^{-1}\mathbf{u}_t^i \tag{78}$$

where $\mathbf{u}_t^i$ is the tangential adjoint velocity in the volume cell i that is adjacent to the location of the surface perturbation. With the same approximation for the primal velocity, we conclude for the cost function variation

$$\mathrm{d}L_{\text{surf}}\propto\mathbf{u}_t^i\cdot\mathbf{v}_t^i \tag{79}$$

DOI: 10.1002/fld

Increasing, on the other hand, the porosity in cell i gives, according to Equation (11), rise to a $\mathrm{d}L_{\mathrm{topo}}$ of

$$\mathrm{d}L_{\mathrm{topo}} \propto \mathbf{u}^i \cdot \mathbf{v}^i = \mathbf{u}_t^i \cdot \mathbf{v}_t^i \tag{80}$$

where the last equality holds because of the vanishing normal velocity components close to the wall. Hence, an inward movement of the surface at a specific position on the wall has a similar impact on the objective function as increasing the porosity in the cell adjacent to this position. Since both geometric changes constitute a 'punishment' of the cell, this result is indeed plausible.

3.1. Example: *Dissipated power*

As a test case for surface sensitivities, we chose a segment of an air duct—a geometry that was well studied in previous works [15, 25]. Figure 4 shows the sensitivities w.r.t. dissipated power for this channel segment. Blue sensitivities correspond to regions where an outward movement of the surface improves the objective function, whereas the reddish patches inside the white contours have to be moved inwards in order to decrease the overall dissipation.

As expected, the by far biggest sensitivities are encountered where the geometric curvature is highest: in the entrance and exit regions of the S-bend. The flow detaches here and gives rise to regions of backflow further downstream. Consequently, the most prominent areas of favourable inward movement are adjacent to those backflow regions.

The sensitivity distributions of Figure 4—specifically, the areas of favourable inward or outward displacement (i.e. the sign of the sensitivity) and the sensitivity peaks in the high-curvature regions—resemble those presented in [25], where the commercial finite-element-based adjoint solver PAMFlow was applied to the same air duct segment.

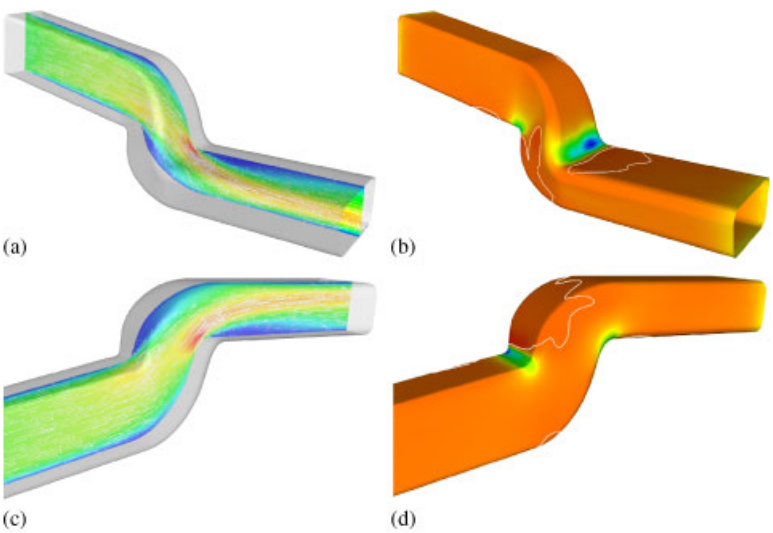

Figure 4. Velocity field inside an air duct segment (a), (c) and sensitivities w.r.t. dissipated power (b), (d): the air enters the channel from the left-hand side at a Reynolds number of 2500. Cold/hot colours on the duct surface mark the areas where an outward/inward surface displacement improves the flow passage. The white contours in (b) and (d) are the isolines of zero sensitivity.

DOI: 10.1002/fld

4. SUMMARY AND OUTLOOK

We derived a continuous adjoint formulation for the steady-state, incompressible Navier–Stokes equations with Darcy porosity term and frozen turbulence. The general form of the adjoint equations and boundary conditions, Equations (20)–(23), was further specialized to the typical primal conditions of ducted flows. Thereby, special emphasis was placed on the cost function versatility of the formulation: While the adjoint equations for ducted flows, Equations (42) and (43), are independent of the objective function by nature—at least as long as the cost function has no contribution from the domain interior, the adjoint boundary conditions, Equations (44)–(48), were expressed in a form that can straightforwardly be adapted to any commonly used objective function.

Using Equations (11) and (76), respectively, the obtained formulation allows one to compute topological and surface sensitivities for ducted flows. Their implementation into the professional finite volume CFD toolbox OpenFOAM was demonstrated for two cost function examples: dissipated power and uniformity of the flow in the outlet plane.

The availability of topological and shape sensitivities inside a professional CFD code and the flexibility of their implementation w.r.t. changes in the objective function is one vital ingredient of the intended composite optimization process chain for freeform geometries [25]: topology optimization for drafting an optimal design from the available installation space and subsequent fine-tuning via shape sensitivities.

The complementary components of this process chain are (1) efficient optimization algorithms to deal with the computed topological and surface sensitivity maps and (2) shape update algorithms to translate the shape sensitivities into a new and smooth shape. For the former, Svanberg's method of moving asymptotes [22] was already identified as a suitable candidate in e.g. [12]. Proposed methods for the latter usually involve mesh morphing, e.g. via a pseudo-shell approach or free-form deformation [26–28]. From the industrial point of view, the most promising method of shape update probably relies on a mapping of the sensitivities onto a CAD parametrization of the geometry, as proposed in [29]. Future work is therefore dedicated to further developing the linkage between surface sensitivities and CAD parametrizations.

REFERENCES

1. Jameson A. *Aerodynamic Shape Optimization Using the Adjoint Method*. VKI Lecture Series, vol. 2. Von Karman Institute: Rhode St Genèse, Belgium, 2003.
2. Giles MB, Pierce NA. An introduction to the adjoint approach to design. *Flow*, *Turbulence and Combustion* 2000; **65**:393.
3. Mohammadi B, Pironneau O. *Applied Shape Optimization for Fluids*. Oxford University Press: Oxford, 2001.
4. Löhner R, Soto O, Yang C. An adjoint-based design methodology for CFD optimization problems. *AIAA-03-0299*, 2003.
5. Soto O, Löhner R. On the computation of flow sensitivities from boundary integrals. *AIAA-04-0112*, 2004.
6. Choi KK, Kim NH. *Structural Sensitivity Analysis and Optimization*, vols. 1 and 2. Springer: Berlin, 2005.
7. Borrvall T, Petersson J. Topology optimization of fluids in Stokes flow. *International Journal for Numerical Methods in Engineering* 2003; **41**:77.
8. Sigmund O, Gersborg-Hansen A, Haber RB. Topology optimization for multi-physics problems: a future FEMLAB application? In *Proceedings of the Nordic MATLAB Conference 2003*, Gregersen L (ed.). Comsol A/S: Søborg, Denmark, 2003; 237.
9. Olesen LH, Okkels F, Bruus H. Topology optimization of Navier–Stokes flow in microfluidics. *ECCOMAS 2004*, Jyväskylä, 2004.

DOI: 10.1002/fld

10. Gersborg-Hansen A, Sigmund O, Haber RB. Topology optimization of channel flow problems. *Structural and Multidisciplinary Optimization* 2005; **30**(3):181.
11. Guest JK, Prévost JH. Topology optimization of creeping flows using a Darcy-Stokes finite element. *International Journal for Numerical Methods in Engineering* 2006; **66**(3):461.
12. Olesen LH, Okkels F, Bruus H. A high-level programming-language implementation of topology optimization applied to steady-state Navier–Stokes flow. *International Journal for Numerical Methods in Engineering* 2006; **65**:975.
13. Srinath DN, Mittal S. A stabilized finite element method for shape optimization in low Reynolds number flows. *International Journal for Numerical Methods in Fluids* 2007; **54**(12):1451–1472.
14. Kaminski T, Giering R, Othmer C. Topological design based on highly efficient adjoints generated by automatic differentiation. *ERCOFTAC Design Optimization Conference*, Las Palmas, 2006.
15. Othmer C, Kaminski T, Giering R. Computation of topological sensitivities in fluid dynamics: cost function versatility. *ECCOMAS CFD 2006*, Delft, 2006.
16. Nadarajah S, Jameson A. A comparison of the continuous and discrete adjoint approach to automatic aerodynamic optimization. *AIAA CP-00-0667*, 2000.
17. Cusdin P, Müller JD. On the performance of discrete adjoint CFD codes using automatic differentiation. *International Journal for Numerical Methods in Fluids* 2005; **47**(6–7):939–945.
18. Griewank A. *Evaluating Derivatives*: *Principles and Techniques of Algorithmic Differentiation*. SIAM: Philadelphia, PA, 2000.
19. OpenFOAM: The Open Source CFD Toolbox. http://www.opencfd.co.uk/openfoam/index.html (2 August 2007).
20. Othmer C, de Villiers E, Weller HG. Implementation of a continuous adjoint for topology optimization of ducted flows. *AIAA-2007-3947*, 2007.
21. Dwight RP, Brezillon J. Effect of various approximations of the discrete adjoint on gradient-based optimization. *AIAA-2006-0690*, 2006.
22. Svanberg K. The method of moving asymptotes—a new method for structural optimization. *International Journal for Numerical Methods in Engineering* 1987; **24**:359.
23. Pironneau O. *Optimal Shape Design for Elliptic Systems*. Springer: Berlin, 1984.
24. Mohammadi B, Bharadwaj R, Molho JI, Santiago JG. Incomplete sensitivities in design and control of fluidic channels. *Annual Research Briefs 2001*, Center for Turbulence Research, Stanford University, Stanford, 2001.
25. Othmer C, Grahs T. Approaches to fluid dynamic optimization in the car development process. *EUROGEN 2005*, Munich, 2005.
26. Samareh JA. A survey of shape parameterization techniques for high-fidelity multidisciplinary shape optimization. *AIAA Journal* 2001; **39**(5):877.
27. Soto O, Löhner R, Yang C. A stabilized pseudo-shell approach for surface parametrization in CFD design problems. *Communications in Numerical Methods in Engineering* 2002; **18**(4):251.
28. Ronzheimer A. Shape parametrization in multidisciplinary design optimization based on freeform deformation. *EUROGEN 2005*, Munich, 2005.
29. Armstrong CG, Robinson TT, Ou H, Othmer C. Linking adjoint sensitivity maps with CAD parameters. *EUROGEN 2007*, Jyväskylä, 2007.

DOI: 10.1002/fld